

# Plumbagin-loaded aptamer-targeted poly D,L-lactic-co-glycolic acid-b-polyethylene glycol nanoparticles for prostate cancer therapy

Minjie Pan, MM<sup>a,b</sup>, Weifeng Li, MM<sup>a,c</sup>, Jun Yang, MD, PhD<sup>a</sup>, Zhiqin Li, MD, PhD<sup>d</sup>, Jun Zhao, MD, PhD<sup>a</sup>, Yajun Xiao, MD, PhD<sup>a</sup>, Yifei Xing, MD, PhD<sup>a</sup>, Xiaoping Zhang, MD, PhD<sup>a</sup>, Wen Ju, MD, PhD<sup>a,\*</sup>

## Abstract

Plumbagin inhibits the growth, metastasis, and invasion of prostate cancer (PCa). However, its lower bioavailability limits biopharmaceutical properties due to insolubility in water. Prostate-specific membrane antigen (PSMA) aptamer-targeted nanoparticles (NPs) significantly enhanced cytotoxicity in prostate epithelial cells. This study aimed to investigate the effects of plumbagin-loaded prostate-specific membrane antigen (PSMA) aptamer-targeted poly D,L-lactic-co-glycolic acid-b-polyethylene glycol (PLGA-PEG) nanoparticles (NPs) on prostate cancer (PCa) in vitro.

PLGA-PEG with a terminal carboxylic acid group (PLGA-PEG-COOH) was synthesized, and plumbagin was loaded on PLGA-PEG-COOH NPs using the nanoprecipitation method and characterized by field emission scanning electron microscopy (SEM), transmission electron microscopy (TEM), and laser light scattering. The uptake and distribution of plumbagin-NPs in human PCa LNCaP cells were investigated by fluorescent labeling. Subsequently, PSMA antibody-targeted PLGA-PEG-COOH NPs (targeted NPs) were prepared by covalent binding and characterized by x-ray photoelectron spectroscopy. Furthermore, the anticancer activity of plumbagin-loaded, targeted NPs was compared with that of nontargeted NPs in LNCaP cells in vitro.

Plumbagin-NPs (diameter of  $189.4 \pm 30.6$  nm and zeta potential of  $-17.1 \pm 3.7$  mV) were optimized based on theoretical drug loading of 5% and a ratio of water:acetone of 3:1. During the first 2 hours, the cumulative release rate of the drug was  $66.4 \pm 8.56\%$ . Moreover, plumbagin-targeted NPs with nitrogen atoms were prepared. The uptake rate was 90% at 0.5 hours for targeted and nontargeted NPs. The  $IC_{50}$  of targeted NPs and nontargeted NPs was  $32.59 \pm 8.03$   $\mu$ M and  $39.02 \pm 7.64$   $\mu$ M, respectively.

Plumbagin-loaded PSMA aptamer-targeted NPs can be used in targeted chemotherapy against PCa.

**Abbreviations:** CRPC = castration-refractory prostate cancer, EE = encapsulation efficiency, HPLC = high-performance liquid chromatography, LLS = laser light scattering, MTT = 3-(4,5-dimethylthiazol-2-yl)-2,5-diphenyltetrazolium bromide, NMR = nuclear magnetic resonance, NP-Ab = conjugation of PSMA antibody to the PLGA-PEG-COOH NPs, NPs = nanoparticles, PCa = prostate cancer, PEG = polyethylene glycol, PLGA = poly D,L-lactic-co-glycolic acid, PLGA-PEG = poly D,L-lactic-co-glycolic acid-b-polyethylene glycol, PLGA-PEG-COOH = PLGA-PEG with a terminal carboxylic acid group, plumbagin-NPs = plumbagin-loaded PLGA-PEG-COOH nanoparticles, PSMA = prostate-specific membrane antigen, SD = standard deviation, SEM = scanning electron microscopy, TEM = transmission electron microscope.

**Keywords:** PLGA-PEG nanoparticles, plumbagin, prostate cancer, prostate-specific membrane antigen

Editor: Sethuramasundaram Pitchaiya.

MP, WL, and JY equally contributed to this study and should be regarded as co-first authors

The authors have no funding and conflicts of interest to disclose.

<sup>a</sup> Department of Urology, Union Hospital, Tongji Medical College, Huazhong University of Science and Technology, Wuhan, <sup>b</sup> Changzhou NO.2 People's Hospital, Changzhou, <sup>c</sup> Department of Urology, Wuhan Medical Care Center for Women and Children, <sup>d</sup> Department of Pharmacy, Tongji Hospital, Tongji Medical College, Huazhong University of Science and Technology, Wuhan, China.

\* Correspondence: Wen Ju, Department of Urology, Union Hospital, Tongji Medical College, Huazhong University of Science and Technology, Wuhan, China (e-mail: weifeng\_ji987@163.com).

Copyright © 2017 the Author(s). Published by Wolters Kluwer Health, Inc. This is an open access article distributed under the terms of the Creative Commons Attribution-Non Commercial-No Derivatives License 4.0 (CCBY-NC-ND), where it is permissible to download and share the work provided it is properly cited. The work cannot be changed in any way or used commercially without permission from the journal.

Medicine (2017) 96:30(e7405)

Received: 5 January 2017 / Received in final form: 8 June 2017 / Accepted: 12 June 2017

<http://dx.doi.org/10.1097/MD.0000000000007405>

## 1. Introduction

In addition to being the most frequently diagnosed cancer, prostate cancer (PCa) is the second leading cause of death among men.<sup>[1]</sup> Androgen deprivation therapy is a common treatment in men with PCa.<sup>[2]</sup> However, it has underlying problems, such as decreased libido, osteopenia with increased fracture risk, and metabolic alterations.<sup>[3]</sup> Recently, docetaxel-based chemotherapy was defined as an effective treatment for patients with castration-refractory PCa (CRPC).<sup>[4]</sup> Nevertheless, the standard chemotherapy against CRPC has some limited efficacy and serious adverse effects because of the unique biological characteristics of PCa. Therefore, new therapeutic strategies are needed.

Plumbagin is the main active ingredient in the traditional Chinese medicine Plumbago. Previous studies have demonstrated that plumbagin played significant roles in inhibiting the growth, metastasis, and invasion of PCa by mediating cellular apoptosis, generation of reactive oxygen species, and a decrease in intracellular glutathione levels.<sup>[5–7]</sup> However, bioavailability of orally administered plumbagin was only 39% due to insolubility in water, which limited biopharmaceutical properties.

Encapsulation of cytotoxic chemotherapeutic agents using biodegradable polymers can improve the efficacy of the treatment and reduce adverse effects of drugs.<sup>[8]</sup> Poly D,L-lactic-co-glycolic acid-polyethylene glycol nanoparticles (PLGA-PEG NPs) have been used to control the release of drugs, which can enhance the effectiveness and safety of drugs.<sup>[9–12]</sup> The prostate-specific membrane antigen (PSMA) is a specific antigen overexpressed on the surface of PCa cell membrane and involves in membrane recycling.<sup>[13]</sup> Docetaxel-loaded PSMA aptamer-targeted NPs in prostate epithelial cells obviously increased cellular toxicity *in vivo* compared with nontargeted NPs.<sup>[14]</sup> However, the efficacy of plumbagin-loaded PSMA aptamer-targeted NPs in PCa therapy is unknown.

In the study, PLGA-PEG with a terminal carboxylic acid group (PLGA-PEG-COOH) was used as the carrier, and plumbagin-loaded PLGA-PEG-COOH NPs were synthesized using the nanoprecipitation method. The formulation and process were optimized based on drug loading and the ratio of water:acetone. Then, the characteristics of NPs, including size, zeta potential, encapsulation efficiency (EE), drug loading, and release, were investigated. Finally, PLGA-PEG-COOH NPs were conjugated to the PSMA aptamer and the efficacy of these NPs in LNCaP cells was assessed. This targeted delivery system could be the foundation for traditional Chinese medicine-based therapies against PCa.

## 2. Materials and methods

### 2.1. Preparation of PLGA-PEG-COOH

PLGA-PEG-COOH (carboxylate-functionalized copolymer) was prepared through the COOH-PEG-NH<sub>2</sub> conjugated to PLGA-COOH according to a previous study.<sup>[15]</sup> In brief, 5 g of PLGA-COOH, which was dissolved in 10 mL of methylene chloride, was first transformed to PLGA-NHS. Then, PLGA-NHS was precipitated with 5 mL of ethyl ether, and the residual NHS was removed using an ice-cold mixture of ethyl ether and methanol. After air-drying, PLGA-NHS was dissolved in 4 mL of chloroform, and 250 mg of NH<sub>2</sub>-PEG-COOH and 28 mg of *N,N*-diisopropylethylamine were added. After precipitation with cold methanol for 12 hours, the residual PEG in co-polymer was removed using the same solvent. The PLGA-PEG block co-polymer was dried under air and stored at 4°C for NPs preparation.

### 2.2. Preparation of plumbagin-loaded PLGA-PEG-COOH NPs

The targeted nanoparticles were synthesized by the nanoprecipitation method.<sup>[16]</sup> In brief, a designated mass ratio of the PLGA-PEG-COOH and plumbagin was dissolved in acetone and subsequently added drop-wise into ultrapure water, while acetone was volatilized overnight. The suspension was centrifuged at the speed of 1500 rpm for 5 minutes twice to remove large particles. Subsequently, the NPs were obtained through centrifuging the supernatant at 12000 rpm for 30 minutes at 4°C to remove excess plumbagin. The NPs were resuspended with adequate volume of water and freeze-dried for further use. For blank NPs, only the polymers were dispersed in acetone.

### 2.3. Determination of particle size and drug content

The NP suspension was diluted using pure water until the counter rate was under 1.5 Mpcs. Then, the size and distribution of NPs were detected using laser light scattering (LLS, Brookhaven Instruments Corporation 90-PLUS analyzer, NY). For drug

content determination, freeze-dried drug-loaded NPs (3 mg) were dispersed in 1 mL of DCM and extracted with 3 mL of acetonitrile and water mixture (v:v, 50:50). The solution was transferred into the high-performance liquid chromatography (HPLC) vial after filtered through a 0.45- $\mu$ m syringe filter. A UV detector (Hitachi, Japan) was used to detect the samples in the HPLC system. In addition, a reverse-phase pentafluorophenyl column (VIVA C18, 150  $\times$  4.6 mm, 5  $\mu$ m) was used. The mobile phase was comprised of water and acetonitrile (50:50, v:v) and kept at a constant flow rate of 1 mL/min. The peak of plumbagin was detected at a wavelength of 245 nm and retention time was obtained at 7 minutes. Its concentration was determined according to the standard curve. The calibration curve was linear between 0.5  $\mu$ g/mL and 200  $\mu$ g/mL. The plumbagin-NPs were characterized by SEM and TEM.

### 2.4. *In vitro* drug release

The plumbagin-NPs (15 mg) were weighed and dispersed into 5 mL of PBS in a dialysis bag. Subsequently, the bag was placed in 50 mL of PBS in a capped bottle, which was shaken in a thermostatic shaker at 37°C and 120 rpm. At allocated time intervals, PBS outside the dialysis bag was piped out into a tube for HPLC analysis and fresh 50 mL of PBS was added to the capped bottle.

### 2.5. Conjugation of anti-PSMA antibody to PLGA-PEG-COOH NPs (NP-Ab) and its characterization

NPs (1 mg) were activated in pure water with EDC and NHS (1:4:4) for 20 minutes at room temperature and redundant EDC and NHS were removed by ultracentrifugation. The NHS-activated NPs (1 mg/mL) were reacted with anti-PSMA (12  $\mu$ g/mL, Abnova Corporation, Taiwan, China) and gently shaken for 120 minutes at room temperature. The resulting NP-Ab was washed using pure water and dissolve in PBS at 4°C until use. The efficacy of NP-Ab was verified by x-ray photoelectron spectroscopy (XPS, Shimadzu Corporation, Kyoto, Japan). The elements on the surface of NP-Ab were assayed based on their specific binding energy from 0 to 1200 eV using pass energy of 80 eV. The nitrogen element was measured by fine mode of 0.5 eV as step.

### 2.6. Cell culture

LNCaP cells were incubated in RMPI 1640 medium with 10% FBS at 37°C in a 5% CO<sub>2</sub> humidified environment. The medium was changed every 2 days and the cells were sub-cultured after reaching confluence.

### 2.7. Cellular uptake *in vitro*

The uptake of NPs by LNCaP cells was verified using the fluorescence experiment. To investigate whether NPs-Ab was located in the LNCaP cells, a green fluorescent probe, coumarin-6, was encapsulated within the NPs by the nanoprecipitation process. PLGA-PEG-COOH (20 mg) was dispersed in acetone (2 mL) containing coumarin-6 (0.01 mg). The solution was stirred using magnetic stirring apparatus for 12 hours and visualized after incubation with LNCaP cells by confocal microscopy. The uptake rate was measured based on the intensity of the fluorescence. LNCaP cells were incubated in black 6-well plates with the NPs encapsulating Rhodamine 123, with or without PSMA, for 0.5, 2, 4, and 6 hours, respectively. The fluorescence intensity was measured by flow cytometry (FCM) at the 487 nm wavelength.

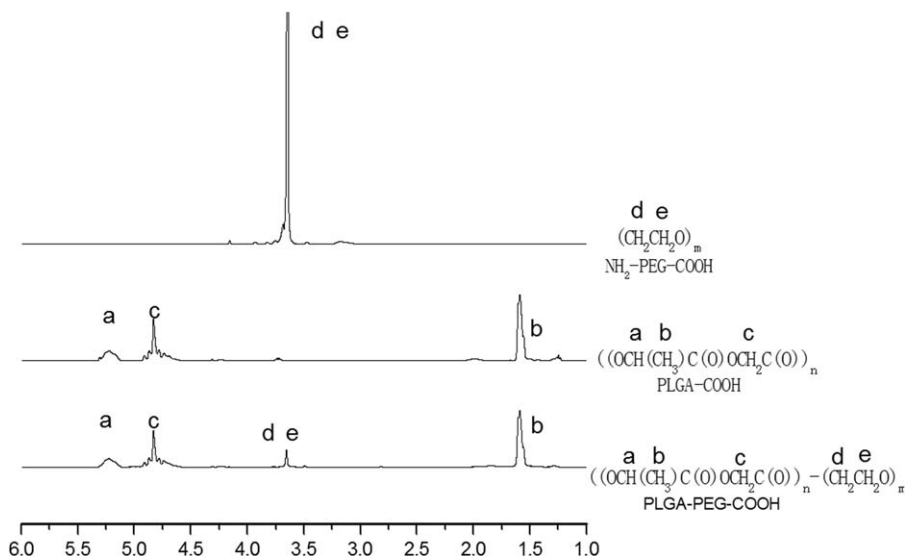


**Figure 1.** <sup>1</sup>H nuclear magnetic resonance spectrum of PEG-PLGA in CDCl<sub>3</sub> at 300 Hz. CDCl<sub>3</sub> = Deuterium chloride, PEG = polyethylene glycol, PLGA = poly D,L-lactic-co-glycolic acid.

**2.8. Cytotoxicity**

Cells were cultured in 96-well plates (10<sup>4</sup> cells/well, 100 μL) overnight. Then, the medium was replaced using samples with different doses for 24, 48, and 72 hours, respectively. Plumbagin was dissolved in dimethyl sulfoxide under the sterilizing station. Cell viability was measured using the 3-(4,5-dimethylthiazol-2-yl)-2,5-diphenyltetrazolium bromide (MTT) assay. The absorbance was assayed by a microplate reader at 570 nm, and the reference wavelength was 620 nm.

**2.9. Statistical analysis**

Data were presented as mean ± standard deviation (SD) from at least 3 measurements using the *t* test and calculated using SPSS 18.0 (SPSS Inc., Chicago, IL). *P* < .05 was considered as statistical significance.

**3. Results**

**3.1. Characterization of PLGA-PEG-COOH**

The PEG content and number-averaged molecular weights of PLGA-PEG-COOH were determined by <sup>1</sup>H nuclear magnetic resonance (NMR, 300 Hz, CDCl<sub>3</sub>) δ 5.3 ppm [m, (OCH(CH<sub>3</sub>)C(O)OCH<sub>2</sub>C(O))<sub>n</sub>-(CH<sub>2</sub>CH<sub>2</sub>O)<sub>m</sub>], 3.7 ppm [s, (OCH(CH<sub>3</sub>)C(O)OCH<sub>2</sub>C(O))<sub>n</sub>-(CH<sub>2</sub>CH<sub>2</sub>O)<sub>m</sub>], 1.6 ppm [d, (OCH(CH<sub>3</sub>)C(O)OCH<sub>2</sub>C(O))<sub>n</sub>-(CH<sub>2</sub>CH<sub>2</sub>O)<sub>m</sub>] (Fig. 1). The characteristic peaks d and e represented the methylene (-CH<sub>2</sub>) of PEG chain, and the characteristic peaks a, b, and c represented the methine (-CH), methyl (-CH<sub>3</sub>), and methylene (-CH<sub>2</sub>) proton of PLGA segment, respectively. From molecular weights of PEG and PLGA, and the ratio of peak area at 5.3 and 3.7 ppm, the average conjugation efficiency between PEG and PLGA was 65%.

**3.2. Optimization of prescription**

On varying the theoretical drug loading (2%, 5%, 10%, 15%) and maintaining the water:solvent ratio (3:1), the particles became larger with the increase in theoretical drug loading (Fig. 2A). Then, we varied the ratio of water:solvent (1:1, 3:1, 5:1, 5:1,

10:1) while the concentration of PLGA-PEG was kept at 10 mg/mL. The particle size did not change significantly when the ratio ≥ 3:1, but EE significantly decreased with an increase in the ratio (Fig. 2B). The optimal formulation had a theoretical drug loading of 5% and water:acetone ratio of 3:1.

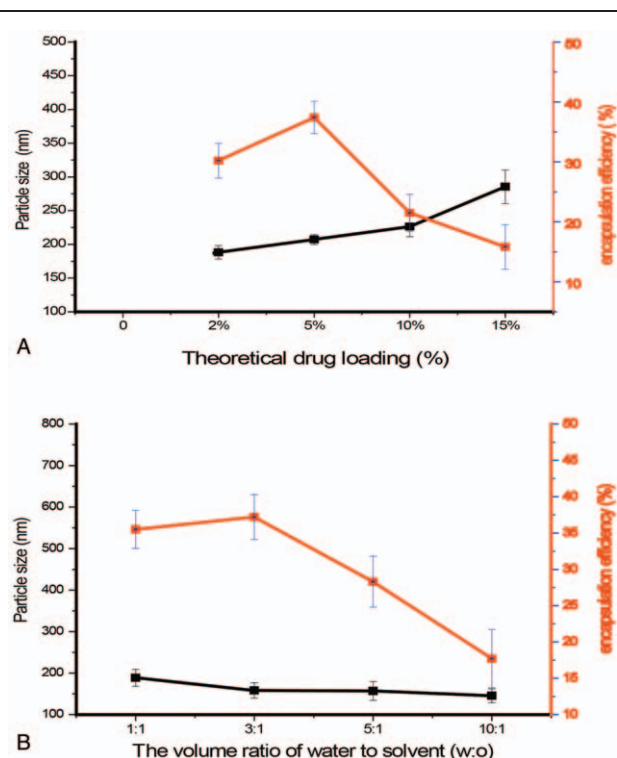


**Figure 2.** Optimization on the preparation of nanoparticles. (A) The size and EE of NPs based on different drug loading (2%, 5%, 10%, and 15%) with the same ratio of water:solvent ratio (3:1). (B) The size and EE of nanoparticles based on varying water:solvent ratios (1:1, 3:1, 5:1, and 10:1) and constant PLGA-PEG polymer concentration (10 mg/mL). EE = encapsulation efficiency, NPs = nanoparticles, PLGA-PEG = poly D,L-lactic-co-glycolic acid-*b*-polyethylene glycol.



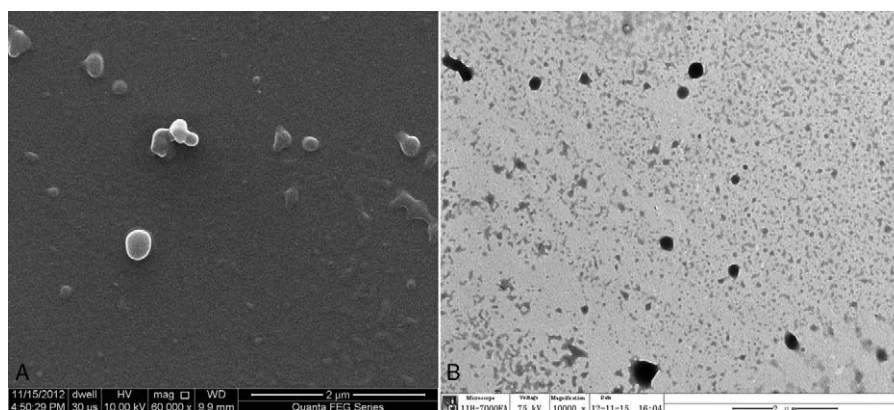


**Figure 3.** Images of plumbagin-loaded nanoparticles with 5% theoretical drug loading observed using (A) the scanning electron microscope and (B) the transmission electron microscope.

### 3.3. Characterization

The resulting NPs had a diameter of  $189.4 \pm 30.6$  nm ( $n=8$ ), with a polydispersity index of  $0.239 \pm 0.095$ . The zeta potential of the NPs was  $-17.1 \pm 3.7$  mV. The morphological appearance of the particles was moderately uniform. The SEM (Fig. 3A) and TEM images (Fig. 3B) of the NPs revealed their regular spherical shape as well as the range of diameters. In addition, there was no significant difference in both size and zeta potential compared with those of NP-Ab ( $P > .05$ ).

### 3.4. In vitro drug release and characterization of NP-Ab

The NPs were released in vitro in 2 phases (Fig. 4A). In the first 2 hours, the drug cumulative release rate ( $66.4 \pm 8.56\%$ ) was rapid. After 2 hours, the drug release increased steadily, the cumulative release rate remained a relatively constant release at 24 hours ( $87.0 \pm 3.08\%$ ). From the first day to the sixth day, sustained release of a small amount of plumbagin was observed, and the cumulative release reached  $90.0 \pm 1.63\%$ .

The XPS N1s region of the plumbagin-NPs before and after conjugation with PMSA antibody revealed that there were nitrogen atoms in plumbagin-NP-Ab and few nitrogen atoms in plumbagin-NPs (Fig. 4B). In addition, no N1s signal was observed for the plumbagin-NP surface.

### 3.5. Lyoprotectant selection

On addition of 10% mannitol, 10% glucose, 10% sucrose, and 10% lactose to nanoparticle suspension and measuring the size and distribution of the prepared nanoparticles using LLS, we found that the addition of 10% sucrose to an aqueous nanoparticle suspension allows recovery of nanoparticles of similar sizes as originally formulated ( $253 \pm 37$  nm, Table 1).

### 3.6. In vitro cellular uptake and uptake efficacy

The fluorescence experiment was performed to study the endocytosis of PLGA-PEG-COOH NPs by LNCaP cells. The result showed that the fluorescence intensity of targeted NPs was stronger than that of nontargeted NPs at the same time (Fig. 5A). In addition, the NPs encapsulating coumarin-6 and showing green fluorescence were accumulated in the cytoplasm, which was stained by the red dye propidium iodide, indicating that LNCaP cells had internalized the NPs. After 0.5, 2, 4, and 6

hours, we found that the uptake rate for targeted NPs (Fig. 5B) and nontargeted NPs (Fig. 5C) was time-dependent and the uptake efficacy was 90% at 0.5 hours.

### 3.7. In vitro cytotoxicity

The cytotoxicity of every type of NP, including NP-loaded drug, NP-unloaded drug, and free drug at different concentrations of 1.25  $\mu$ M, 2.5  $\mu$ M, 5  $\mu$ M, 10  $\mu$ M, and 20  $\mu$ M. The  $IC_{50}$  of each

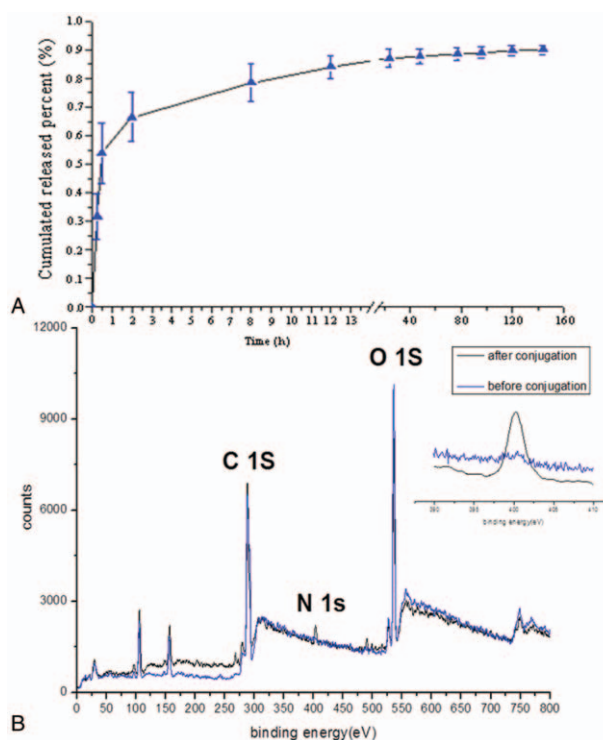


**Figure 4.** The release profile of plumbagin-loaded PLGA-PEG-COOH nanoparticles in vitro (A) and conjugation of anti-PSMA antibody to NPs (B). The blue line indicates the x-ray photoelectron spectroscopy (XPS) spectrum of plumbagin-loaded NPs, and the black line indicates the XPS spectrum of plumbagin-loaded NPs after conjugation with antibody. The insert indicates the nitrogen signal at high resolution. NPs = nanoparticles, PLGA-PEG-COOH = PLGA-PEG with a terminal carboxylic acid group, PSMA = prostate-specific membrane antigen, XPS = x-ray photoelectron spectroscopy.

**Table 1****Effect of lyoprotectant prior to lyophilization on nanoparticles size.**

	Blank	10% Mannitol	10% Glucose	10% Sucrose	10% lactose
Suspended before freeze-dried, nm	210	210	210	210	210
Re-suspended after freeze-dried, nm	Coagulation	340±50	3000±1260	253±37	4500±1778

group has been presented in Fig. 6. The cytotoxicity of targeted and nontargeted NPs without encapsulating drugs were negligible; the  $IC_{50}$  of targeted NP-unloaded drug and nontargeted NP-unloaded drug was  $32.59 \pm 8.03 \mu M$  and  $39.02 \pm 7.64 \mu M$ , respectively. The NP-loaded drug and free drug could induce cytotoxicity dose-dependently. However, the  $IC_{50}$  of free drug was  $1.74 \pm 0.22 \mu M$ , which was lower than that of targeted NPs and nontargeted NPs ( $4.78 \pm 0.83 \mu M$  and  $10.33 \pm 2.48 \mu M$ , respectively). From  $IC_{50}$  value of each group, we determined that the cytotoxicity of targeted NP-loaded drug was twice that of nontargeted NP-loaded drug in LNCaP cells.

#### 4. Discussion

We optimized drug-loaded nanoparticle formulation using 3 key indicators: particle size, EE, and drug loading. Cheng et al<sup>[15]</sup> developed NPs using the PLGA-PEG-COOH polymer and studied the effects of altering formulation parameters, such as polymer concentration, miscibility of water and solvent, theoretical drug loading, and the ratio of water and solvent,

on the size of NPs. In the current study, we referred to the results of their experiments and made some modifications according to the characteristics of our own trials. We chose acetone as the organic solvent and set polymer concentration at 10 mg/L. We found the optimal prescription to have a theoretical drug loading of 5% and water:acetone ratio of 3:1.

Particle magnitude plays an important role in the biodistribution of NPs. Studies on liposomes demonstrated that splenic sequestration of particles decreased linearly with decreasing particle size.<sup>[17,18]</sup> Smaller particles make intravenous injection easier and sterilization simpler by filtration.<sup>[19,20]</sup> Drug EE is another factor to be considered for plumbagin. The drugs encapsulated by NPs are soluble in water, even completely soluble in water.<sup>[21]</sup> However, plumbagin is slightly soluble in water. Therefore, improving the EE becomes difficult. We made many attempts to reduce the drug solubility in the external water phase to increase the rate of encapsulation and found that less external water phase had better effects, which led to higher theoretical drug loading. In addition, we attempted to improve EE based on the physical and chemical properties of the drug.

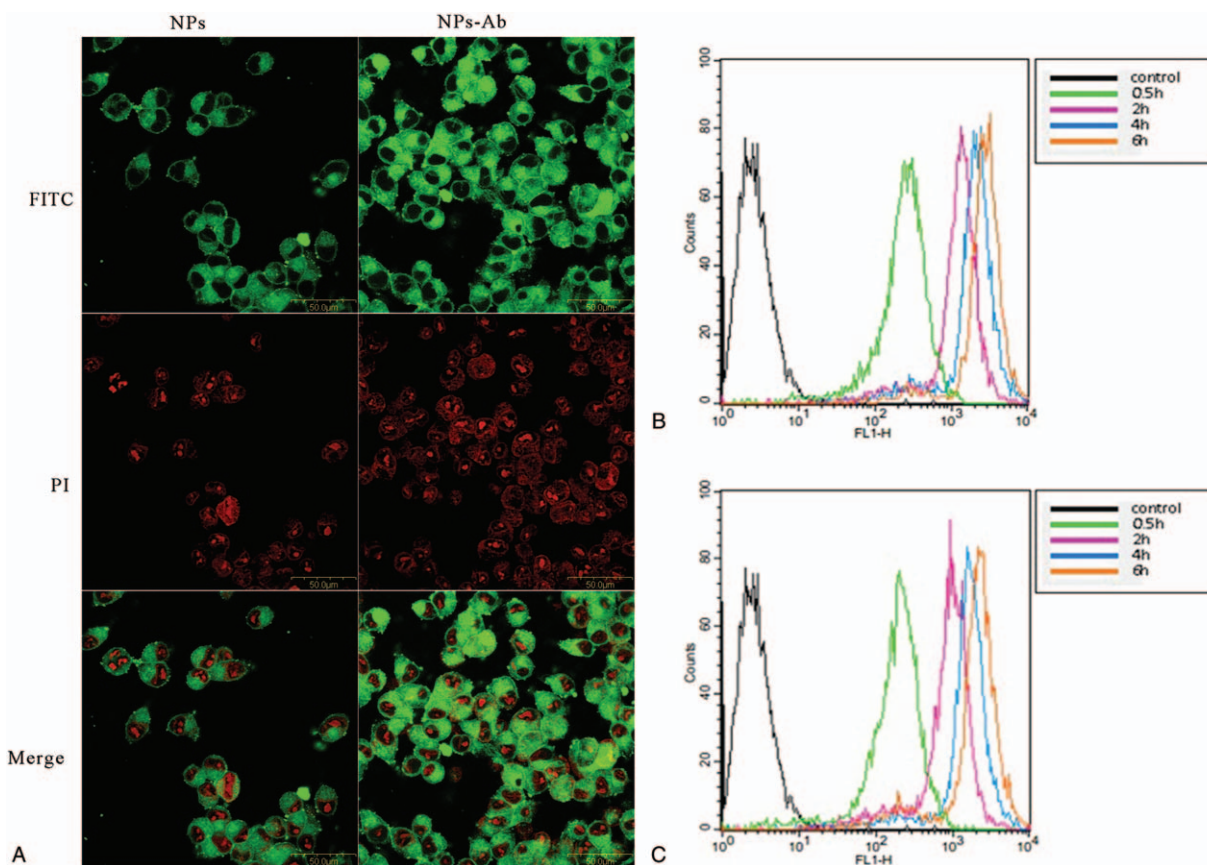


**Figure 5.** (A) Green fluorescent dye coumarin-6 co-encapsulated in PLGA-PEG-COOH nanoparticles (NPs). (B) The uptake efficacy of targeted NPs by LNCaP cells. (C) The uptake efficacy of non-targeted NPs by LNCaP cells. The nucleus was visualized in red by propidium iodide analysis. NP = nanoparticles, PI = propidium iodide, FITC = fluorescein isothiocyanate, PLGA-PEG-COOH = PLGA-PEG with a terminal carboxylic acid group.

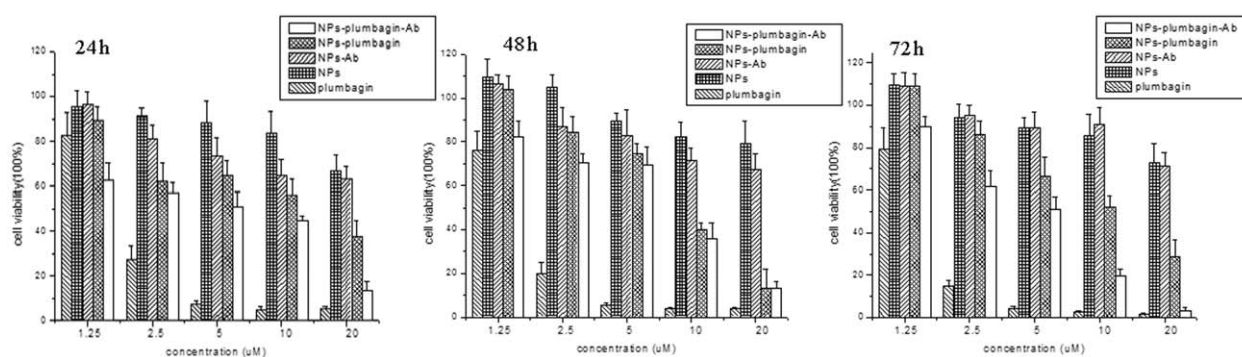


**Figure 6.** Cytotoxicity of LNCaP cells treated with NPs, plumbagin, plumbagin-NP, NP-Ab, and plumbagin-NP-Ab at different concentrations (1.25  $\mu\text{M}$ , 2.5  $\mu\text{M}$ , 5  $\mu\text{M}$ , 10  $\mu\text{M}$ , and 20  $\mu\text{M}$ ) after 24h, 48h, and 72h. Cells were treated with RPMI-1640 as control. All results are expressed as the mean percentage of control  $\pm$  SD of quadruplicate determinations from 3 independent experiments. NPs-Ab = conjugation of PSMA antibody to the PLGA-PEG-COOH NPs, plumbagin-NP = plumbagin-loaded PLGA-PEG-COOH nanoparticles, plumbagin-NP-Ab = plumbagin-loaded NPs-Ab.

According to the molecular structure and pH test strip, the aqueous solution of plumbagin is acidic. Therefore, we tried to reduce its solubility in the water phase by varying the pH of the external phase (pH=3, 4, 5, 6, 7) or adding salt to the external phase. In addition, we varied the theoretical drug loading (2%, 5%, 10%, 15%), and maintained the water:solvent ratio at 3:1. The particles became larger with the increase in theoretical drug loading. We also found that too small or too large theoretical drug loading leads to poor EE and that the optimum point was 5%.

Zeta potential plays an important role in the particle stability through the electrostatic repulsion between the particles. Zeta potential of PLGA NPs is approximately 50 mV.<sup>[22]</sup> The main reason for the decrease in the absolute value of the zeta potential was that most of the surface of the NPs was covered by nonionic PEG.

The burst release of drug may be the reason for the drug being adsorbed at the surface of the polymer, which easily diffused at the initial incubation time.<sup>[23]</sup> Compared with the release profile of gemcitabine from PLGA NPs in a previous study, in which  $6.93 \pm 1.00\%$  of drug was released within the initial 0.5 hours and  $36.9 \pm 1.10\%$  was released in 48 hours,<sup>[24]</sup> we found that in the first 2 hours, the cumulative release rate of the drug was  $66.4 \pm 8.56\%$ . This facilitated release may be ascribed to low water solubility of the drug. In brief, the plumbagin on the surface of the NPs rapidly dissolved into the water, resulting in a sudden release. When water passed through the pores of NPs, the outer plumbagin was dissolved and slow released. Finally, plumbagin in the core was gradually released by the degradation of NPs.

After examining the cytotoxicity of every type of NP at different concentrations, we found that the  $\text{IC}_{50}$  of targeted NP-unloaded drug and nontargeted NP-unloaded drug was  $32.59 \pm 8.03 \mu\text{M}$  and  $39.02 \pm 7.64 \mu\text{M}$ , respectively, which indicates low cytotoxicity and attributes to our polymer system.<sup>[25]</sup> The NP-loaded drug and free drug were cytotoxic in a dose-dependent manner. Although the  $\text{IC}_{50}$  of free drug was  $1.74 \pm 0.22 \mu\text{M}$ ,<sup>[7]</sup> lower than that of targeted NPs and nontargeted NPs ( $4.78 \pm 0.83 \mu\text{M}$  and  $10.33 \pm 2.48 \mu\text{M}$ , respectively), NP-loaded drug had long circular half-life and reduced the adverse effects of free drug by releasing the drug inside of cells. From  $\text{IC}_{50}$  values of each group, the cytotoxicity of targeted NP-loaded drug were found to be twice that of nontargeted NP-loaded drug in LNCaP cells, which suggested that targeted NP-loaded drug is beneficial.

In conclusion, the release curve of targeted NPs revealed that plumbagin could be released through 2 phases (sudden release and sustained release for a long period), thereby enhancing the anticancer activity of plumbagin. Therefore, plumbagin-loaded

PSMA aptamer-targeted NPs can be used in targeted chemotherapy against PCa.

## References

- [1] Siegel R, Naishadham D, Jemal A. Cancer statistics, 2013. *CA Cancer J Clin* 2013;63:11–30.
- [2] Segal RJ, Reid RD, Courneya KS, et al. Resistance exercise in men receiving androgen deprivation therapy for prostate cancer. *J Clin Oncol* 2003;21:1653–9.
- [3] Sharifi N, Gulley JL, Dahut WL. Androgen deprivation therapy for prostate cancer. *JAMA* 2005;294:238–44.
- [4] Loriot Y, Massard C, Gross-Goupil M, et al. The interval from the last cycle of docetaxel-based chemotherapy to progression is associated with the efficacy of subsequent docetaxel in patients with prostate cancer. *Eur J Cancer* 2010;46:1770–2.
- [5] Aziz MH, Dreckschmidt NE, Verma AK, et al. A medicinal plant-derived naphthoquinone, is a novel inhibitor of the growth and invasion of hormone-refractory prostate cancer. *Cancer Res* 2008;68:9024–32.
- [6] Hafeez BB, Zhong W, Fischer JW, et al. Plumbagin, a medicinal plant (*Plumbago zeylanica*)-derived 1, 4-naphthoquinone, inhibits growth and metastasis of human prostate cancer PC-3M-luciferase cells in an orthotopic xenograft mouse model. *Mol Oncol* 2013;7:428–39.
- [7] Powolny AA, Singh SV. Plumbagin-induced apoptosis in human prostate cancer cells is associated with modulation of cellular redox status and generation of reactive oxygen species. *Pharm Res* 2008;25:2171–80.
- [8] Kumari A, Yadav SK, Yadav SC. Biodegradable polymeric nanoparticles based drug delivery systems. *Colloids Surf B Biointerfaces* 2010;75:1–8.
- [9] 2011; Song Z, Feng R, Sun M, et al. Curcumin-loaded PLGA-PEG-PLGA triblock copolymeric micelles: preparation, pharmacokinetics and distribution in vivo, *Journal of colloid and interface science*. 354:116–23.
- [10] Chen S, Singh J. Controlled release of growth hormone from thermosensitive triblock copolymer systems: in vitro and in vivo evaluation. *Int J Pharm* 2008;352:58–65.
- [11] Khalil NM, do Nascimento TCF, Casa DM, et al. Pharmacokinetics of curcumin-loaded PLGA and PLGA-PEG blend nanoparticles after oral administration in rats. *Colloids Surf B Biointerfaces* 2013;101:353–60.
- [12] Anganeh MT, Mirakabad FST, Izadi M, et al. The comparison between effects of free curcumin and curcumin loaded PLGA-PEG on telomerase and TRF1 expressions in calu-6 lung cancer cell line. *Int J Biosci* 2014;4:134–45.
- [13] Ghosh A, Heston WD. Tumor target prostate specific membrane antigen (PSMA) and its regulation in prostate cancer. *J Cell Biochem* 2004;91:528–39.
- [14] Farokhzad OC, Cheng J, Teply BA, et al. Targeted nanoparticle-aptamer bioconjugates for cancer chemotherapy in vivo. *Proc Natl Acad Sci USA* 2006;103:6315–20.
- [15] Cheng J, Teply BA, Sherifi I, et al. Formulation of functionalized PLGA-PEG nanoparticles for in vivo targeted drug delivery. *Biomaterials* 2007;28:869–76.
- [16] 2002; Chorny M, Fishbein I, Danenberg HD, et al. Lipophilic drug loaded nanospheres prepared by nanoprecipitation: effect of formulation variables on size, drug recovery and release kinetics, *Journal of controlled release*. 83:389–400.

- [17] Storm G, Bellior SO, Daemen T, et al. Surface modification of nanoparticles to oppose uptake by the mononuclear phagocyte system. *Adv Drug Deliv Rev* 1995;17:31–48.
- [18] Litzinger DC, Buiting AM, van Rooijen N, et al. Effect of liposome size on the circulation time and intraorgan distribution of amphipathic poly (ethylene glycol)-containing liposomes. *Biochim Biophys Acta* 1994;1190:99–107.
- [19] Kwon GS, Kataoka K. Block copolymer micelles as long-circulating drug vehicles. *Adv Drug Deliv Rev* 1995;16:295–309.
- [20] Konan YN, Gurny R, Allémann E. Preparation and characterization of sterile and freeze-dried sub-200nm nanoparticles. *Int J Pharm* 2002;233:239–52.
- [21] Monteiller C, Lang T, Macnee W, et al. The pro-inflammatory effects of low-toxicity low-solubility particles, nanoparticles and fine particles, on epithelial cells in vitro: the role of surface area. *Occup Environ Med* 2007;64:609–15.
- [22] Govender T, Stolnik S, Garnett MC, et al. PLGA nanoparticles prepared by nanoprecipitation: drug loading and release studies of a water soluble drug. *J Control Release* 1999;57:171–85.
- [23] Asadishad B, Vossoughi M, Alamzadeh I. In vitro release behavior and cytotoxicity of doxorubicin-loaded gold nanoparticles in cancerous cells. *Biotechnol Lett* 2010;32:649–54.
- [24] Aggarwal S, Gupta S, Pabla D, et al. Gemcitabine-loaded PLGA-PEG immunonanoparticles for targeted chemotherapy of pancreatic cancer. *Cancer Nanotechnol* 2013;4:145–57.
- [25] Gryparis EC, Hatzia Apostolou M, Papadimitriou E, et al. Anticancer activity of cisplatin-loaded PLGA-mPEG nanoparticles on LNCaP prostate cancer cells. *Eur J Pharm Biopharm* 2007;67:1–8.